

^{1,*} Bo Xu
²Shun Li
³Luyao Yuan
⁴Hao Yu
⁵Yanchao Li

Model Prediction and Optimization of Belt Drive System Vibration Suppression Based on Industrial Robot Joints



Abstract: - Addressing the vibration issues caused by torsional angle changes in the belt transmission systems of industrial robots during practical applications, this paper introduces a control strategy that integrates a Model Predictive Control (MPC) compensation mechanism. By applying the Lagrangian method, a dynamic mathematical model correlating torsional angle and torque was established, and an algorithm design combining MPC with its compensatory controller was developed. This strategy was validated in a MATLAB simulation environment. Simulation results demonstrate that, compared to traditional sliding mode control, the newly proposed controller significantly improved response speed in tracking the torsional angle's position and angular velocity, achieving enhancements of approximately 2 seconds and 1 second, respectively. This led to higher tracking accuracy and faster convergence speed, effectively enhancing the vibration suppression performance of industrial robot joint belt transmission systems.

Keywords: Industrial Robot, Belt Drive, Torsional Angle, MPC, Vibration Suppression.

I. INTRODUCTION

With the steady advancement of "Industry 4.0" and "Made in China 2025," industrial robots have begun to find applications in the engineering equipment sector (as depicted in Figure 1, a drill pipe stacking robot developed by China University of Geosciences).



Figure 1: Drill Pipe Stacker

Compared to traditional engineering equipment, the application of industrial robots in the construction machinery industry has attracted significant attention due to advantages such as short development cycles and strong adaptability. However, engineering equipment in this industry is often used in scenarios involving heavy loads and harsh environments, posing challenges to the performance of robots. During loading or unloading operations, the influence of the end effector often causes vibration phenomena, which not only reduces the control accuracy of the robot but also severely impacts its operational efficiency. In some cases, mechanical vibrations during the loading process can even cause irreversible damage to the robot's transmission system and the workpieces being manipulated. Therefore, investigating the causes of end-effector vibrations and developing effective vibration control algorithms have become key technical challenges for the application of industrial robots in construction machinery [1].

In recent years, with the continuous improvement of industrial automation levels, the application of industrial robots has become increasingly widespread, and optimizing and enhancing their performance has emerged as a hot topic of research. Particularly, the issue of vibration generated by industrial robots during precision operations has attracted considerable attention from scholars. Specifically, the fifth and sixth joints of industrial robots often employ a belt-drive structure (as shown in Figure 2), which, although offers certain

¹ Beijing Information Science and Technology University, Beijing, 100096, China

² Beijing University of Information Technology, Beijing, 100096, China

³ Beijing Information Science and Technology University, Beijing, 100096, China

⁴ Beijing Information Science and Technology University, Beijing, 100096, China

⁵ Beijing Information Science and Technology University, Beijing, 100096, China

*Corresponding author: Bo Xu

Copyright © JES 2024 on-line : journal.esrgroups.org

flexibility and adaptability, also introduces a key factor leading to vibrations at the end-effector due to the relatively lower stiffness of belt drives.

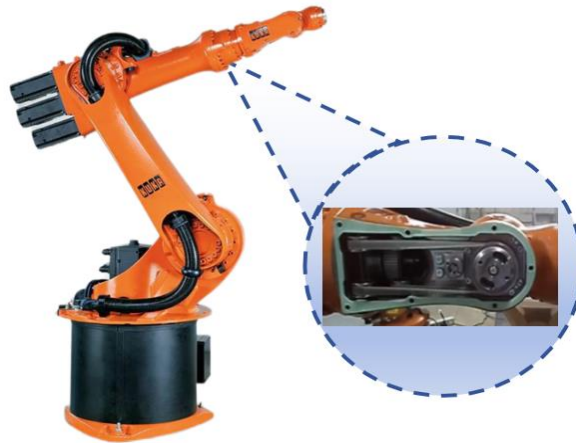


Figure 2: Belt Drive Diagram of an Industrial Robot Transmission System

The application of industrial robots in high-precision operation fields is increasing, making vibration control one of the key technical challenges to enhance their performance. Traditional vibration control methods, such as design improvements through mathematical modeling followed by finite element analysis or the addition of damping vibration reduction components, have been widely applied. Additionally, classical control techniques, such as PD/PID or sliding mode control, also play an important role in the vibration suppression of industrial robots. However, these methods still face certain limitations when dealing with vibrations caused by flexible loads. Hu Junyu proposed a vibration suppression algorithm for flexible loads, which is based on a preset transfer function and recursive least squares method for iterative optimization. By accurately calculating the vibration suppression parameters, the accuracy of vibration control has been significantly improved [2]. Liu He addressed the issue of residual vibration caused by the flexibility of industrial robot joints during high-speed movement by designing multiple notch filters in the controller to effectively filter out resonance signals [3]. Zhang Tie proposed a vibration suppression method based on input shaping to effectively mitigate residual vibrations of flexible loads induced by sudden changes in motion states and internal components' flexibility in a six-degree-of-freedom industrial robot [4]. Dongwon Shin and Wisnu Aribowo separately achieved vibration suppression through considerations of natural frequencies and cubic spline optimization [5,6], while Oh-Hara S designed a gain scheduling control strategy for achieving high-speed transfers and high-precision positioning [7]. Despite these advancements, research on addressing vibration issues in belt drive systems using Model Predictive Control (MPC) technology is relatively scarce.

Model Predictive Control (MPC) represents a sophisticated control paradigm, predicated on the utilization of predictive models to refine the efficacy of current control measures. Central to this approach is the iterative computation of forthcoming control inputs at each decision juncture, predicated on forecasts of the system's imminent state, thereby aiming to minimize a cost function delineated over prospective behaviors. This necessitates a prognosticative analysis of the system's future dynamics, typically facilitated through the application of a rigorously defined mathematical model. MPC's distinct advantage lies in its adeptness at navigating the intricacies of systems characterized by multivariate dynamics, inherent constraints, and nonlinear behaviors. It is uniquely capable of accommodating both input and output constraints, seamlessly integrating these considerations during the design phase to ensure operations remain confined within the realms of safety and predefined technical parameters. Furthermore, MPC's strategy of optimizing forecasted performance across a temporal horizon, as opposed to a singular focus on the immediate future, culminates in more refined control actions and an augmentation of system stability. The versatility of MPC's application spectrum is remarkably extensive, spanning domains such as chemical processing, energy management, automotive systems, and robotics, to name a few. It plays an instrumental role in bolstering the safety, operational efficiency, and reliability of sophisticated industrial operations. When juxtaposed with traditional nonlinear control methodologies, MPC exhibits superior efficiency and adaptability in mitigating vibrational phenomena in belt transmission systems, thereby underscoring its pivotal role in contemporary control theory and application.

This study designed a controller based on Model Predictive Control (MPC), forming a comprehensive belt vibration suppression strategy in comparison with sliding mode control. By considering the impact of different viscous damping coefficients and integrating the time-domain parameters application of MPC, an adaptive time-

domain parameter switching scheme was proposed. Simulation analysis was conducted using Simulink, and the results were compared with the sliding mode control method. The effectiveness of the proposed method was demonstrated, validating the correctness of the control strategy and further confirming the superior performance of MPC in the vibration control of industrial robots. This optimization scheme not only clarified the research progress and practical application value of various vibration suppression technologies but also highlighted the broad application prospects and significant importance of MPC in the field of vibration control for industrial robots. It provides new ideas and methods for the precise control and application of future industrial robots.

II. BELT DRIVE MODEL

A. Schematic Diagram

The system consists of two rigid pulleys connected by a belt made of a non-linear viscoelastic material. The structural schematic of the system is as illustrated in Figure 3. The radius of the drive pulley is r_1 , with a rotational inertia of J_1 ; the radius of the driven pulley is r_2 , with a rotational inertia of J_2 ; The moment of inertia of the harmonic torque applied to the driving pulley is shown in equation (1).

$$L_{\text{Sum}} = L_1 + L_2 + L_3 = \sqrt{a^2 + (r_2 - r_1)^2} + \pi(r_1 + r_2), \quad (1)$$

where a represents the center distance between the pulleys in the belt drive theory, and the total length of the belt is θ_1 . and θ_2 denote the rotational angles of the driving and driven pulleys, respectively.

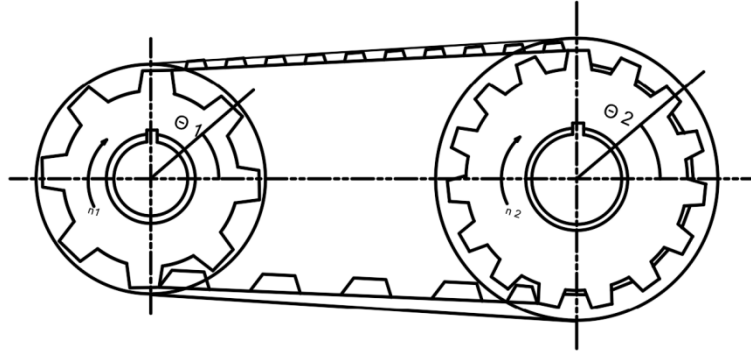


Figure 3: Schematic Diagram of the Belt Drive System for an Industrial Robot Joint

To establish the Lagrangian dynamics model of a belt drive system, we begin by identifying the system's kinetic energy (T) and potential energy (V). ξ represents the belt's absolute elongation during operation, c denotes the coefficient of viscous damping, k' is the quadratic non-linear stretch elasticity parameter of the belt, and k represents the cubic non-linear stretch elasticity parameter. τ stands for the generalized torque. The Lagrangian dynamics equation is as follows:

$$L = T - V \quad (2)$$

$$\frac{d}{dt} \left(\frac{\partial L}{\partial \dot{q}_\alpha} \right) - \frac{\partial L}{\partial q_\alpha} = 0 \quad (3)$$

$$T = \frac{1}{2} J_1 \dot{\theta}_1^2 + \frac{1}{2} J_2 \dot{\theta}_2^2 \quad (4)$$

$$V = (2K_1)(r_1\theta_1 - r_2\theta_2)^2/2 + (2k'K_1)(r_1\theta_1 - r_2\theta_2)^3/3 + (2kK_1)(r_1\theta_1 - r_2\theta_2)^4/4 \quad (5)$$

Let E represent the elastic modulus of the belt, and denote the cross-sectional area of the belt. The linear stretching stiffness of the belt (K_1) can be obtained as follows:

$$K_1 = \frac{EA}{L_{\text{Sum}}} \quad (6)$$

Based on the Lagrange equation, the torques of the driving and driven pulleys are as follows:

$$\tau_1 = \frac{d}{dt} \frac{\partial T}{\partial \dot{\theta}_1} - \frac{\partial T}{\partial \theta_1} + \frac{\partial V}{\partial \theta_1} = J_1 \ddot{\theta}_1 + 2K_1 r_1 (r_\theta + k' r_\theta^2 + k_1 r_\theta^3) \quad (7)$$

$$r_\theta = r_1 \theta_1 - r_2 \theta_2 \quad (8)$$

$$\tau_2 = \frac{d}{dt} \frac{\partial T}{\partial \dot{\theta}_2} - \frac{\partial T}{\partial \theta_2} + \frac{\partial V}{\partial \theta_2} = J_2 \ddot{\theta}_2 - 2K_1 r_2 (r_\theta + k' r_\theta^2 + k_1 r_\theta^3) \quad (9)$$

$$\begin{aligned} \begin{pmatrix} \tau_1 \\ \tau_2 \end{pmatrix} &= \begin{pmatrix} J_1 & 0 \\ 0 & J_2 \end{pmatrix} \begin{pmatrix} \ddot{\theta}_1 \\ \ddot{\theta}_2 \end{pmatrix} + \begin{pmatrix} 2K_1 r_1 [r_\theta + k' r_\theta^2 + k_1 r_\theta^3] \\ -2K_1 r_2 [r_\theta + k' r_\theta^2 + k_1 r_\theta^3] \end{pmatrix} \\ &= \begin{pmatrix} M_0 - 2c r_1 r_\theta \\ 2c r_2 r_\theta \end{pmatrix} = \begin{pmatrix} M_0 \\ 0 \end{pmatrix} + \begin{pmatrix} -2c r_1 r_\theta \\ 2c r_2 r_\theta \end{pmatrix} \end{aligned} \quad (10)$$

Let $\alpha = \theta_1 - \frac{r_2}{r_1}\theta_2$ signify the establishment of a torsional angle. The objective is to transform the system of equations concerning torsional angles θ_1 and θ_2 into a torsional vibration equation with respect to the torsional angle α .

$$\ddot{\alpha} - 2\mu\dot{\alpha} + w_0^2\alpha + k_2\alpha^2 + k_3\alpha^3 = J_2u \quad (11)$$

Wherein,

$$\begin{cases} w_0 = \frac{2K_1(r_1^2J_2+r_2^2J_1)}{J_1J_2} \\ 2\mu = \frac{2c(r_1^2J_2+r_2^2J_1)}{J_1J_2} \\ k_1 > 0 \\ k_2 = \frac{2K_1kr_1(r_1^2J_2-r_2^2J_1)}{J_1J_2} \\ k_3 = \frac{2K_1kr_1^2(r_1^2J_2+r_2^2J_1)}{J_1J_2} \end{cases} \quad (12)$$

The analysis above indicates that internal viscous damping is the primary cause of vibration within the system. This form of damping results from energy dissipation due to resistance proportional to the velocity and force magnitude as the vibrating system moves, leading to the loss of some vibrational energy under the effect of resistance, which is eventually converted into heat energy. Consequently, variations in the viscous damping coefficient have a direct impact on the system's torsional angle. In the process of controlling vibration, adjusting the damping coefficient becomes a key measure, as selecting an appropriate damping coefficient can effectively reduce the vibration intensity of the system. Therefore, in designing vibration control systems, precise control of the damping coefficient can effectively regulate the system's dynamic response, thereby reducing the amplitude and frequency of vibration. This requires not only a deep understanding of the system's dynamic characteristics but also consideration in the design of control strategies on how to optimize system performance by adjusting the damping coefficient to achieve effective vibration suppression. This approach has been proven theoretically and practically effective in reducing vibrations in belt drive systems, playing a significant role in enhancing the stability and operational efficiency of mechanical systems.

The general form of the nonlinear dynamic model for a robotic arm can be derived as follows:

$$\begin{cases} M(q)\ddot{q} + C(q, \dot{q})\dot{q} = \tau \\ \ddot{\alpha} - 2\mu\dot{\alpha} + w_0^2\alpha + k_2\alpha^2 + k_3\alpha^3 = J_2u \end{cases} \quad (13)$$

Wherein,

$$\begin{cases} M = I \\ C = -2\mu \\ \tau = J_2u - (w_0^2\alpha + k_2\alpha^2 + k_3\alpha^3) \end{cases} \quad (14)$$

With a constant torque $J_2u \gg (w_0^2\alpha + k_2\alpha^2 + k_3\alpha^3)$, and aiming to suppress the belt's vibration by having the torsional angle α approach zero (not considering external disturbances). The control vector is denoted as $\tau = J_2u$, and the output vector as $y = q$. The state equation can be formulated as follows:

$$\begin{cases} \dot{x} = f(x, u) \\ f(x, u) = \begin{bmatrix} \dot{q} \\ \ddot{q} \end{bmatrix} = \begin{bmatrix} \dot{q} \\ M_{\parallel}^{-1}(\tau - C\dot{q}) \end{bmatrix} = \begin{bmatrix} f_1 \\ f_2 \end{bmatrix} \end{cases} \quad (15)$$

III. Model Predictive Design for Suppression of Torsional Vibration in Belt Drives

The core of the Model Predictive Control (MPC) algorithm lies in utilizing the system model to predict and determine a series of future optimal control inputs based on the current state and a set of given control inputs, aiming to achieve the optimal state at the next moment. This process involves setting a prediction horizon N , tracking a reference trajectory r_k , and achieving system control by minimizing a cost function while satisfying constraints. At time k , the cost function considers the tracking error e_k (the error between the system output and the reference trajectory r_k) and the control input u_k . By forecasting N steps ahead, MPC calculates the optimal sequence of control inputs. These control inputs are designed to minimize the cost function, thereby realizing optimal control of the system [8-12].

B. Linear Discretization of Continuous Nonlinear Systems

In traditional Model Predictive Control (MPC), discrete-time linear models are employed. To address issues when dealing with nonlinear continuous systems, traditional MPC strategies are often based on discrete-time linear models. However, most real-world dynamic systems exhibit nonlinear and continuous characteristics,

which limit the direct application of conventional MPC methods. To overcome this challenge, successive linearization techniques have been introduced [13-15]. The main idea behind successive linearization is to perform a linearization operation on the nonlinear continuous system at each current state's time point. The linearized system is then transformed into a discrete form, allowing its application within the MPC framework by converting it into predictive equations, thereby enabling effective prediction and control of the system.

C. Design of Vibration Suppression Controller

The structure of the vibration suppression controller is illustrated in Figure 4:

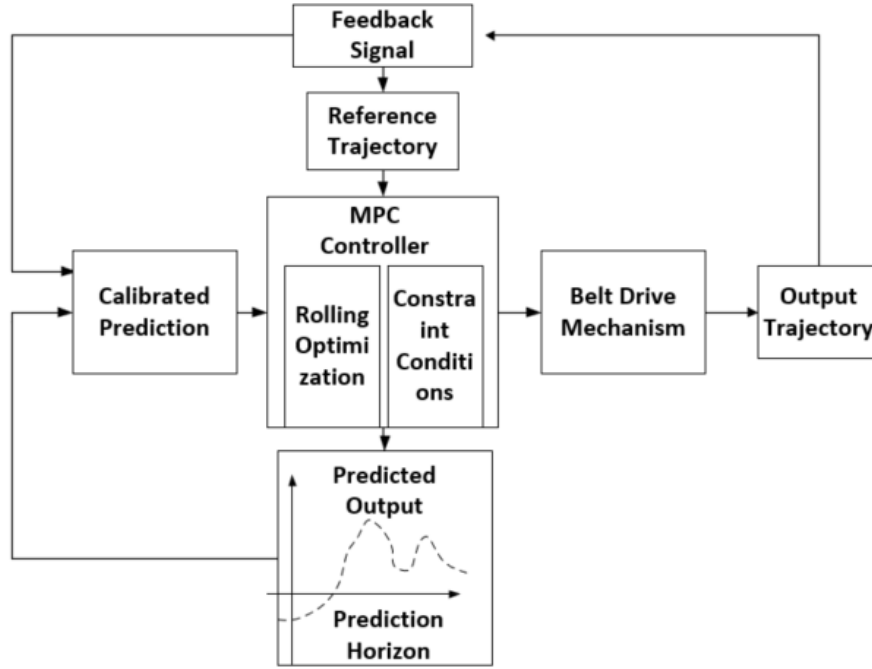


Figure 4: Structure of the Vibration Suppression Controller

By performing a Taylor expansion at the reference point (x_r, u_r) and subtracting the reference trajectory, we can obtain:

$$\tilde{x}_k = \dot{x}_k - \dot{x}_r = f x + f u \tag{16}$$

$$f x = \frac{\partial f(x_{k-1}, u_k)}{\partial x_{k-1}} (x_{k-1} - x_r) \tag{17}$$

$$f u = \frac{\partial f(x_{k-1}, u_k)}{\partial u_k} (u_k - u_r)$$

$\tilde{x} = (\tilde{x}_k - \tilde{x}_r)/T$, To proceed with discretization:

Please see last page of this document for AN EXAMPLE of a 2-COLUMN Figure.

$$\tilde{x}_k = A_1 \tilde{x}_{k-1} + B_1 \tilde{u}_k \tag{18}$$

The Jacobian submatrix of the derivative functions of the state components is as follows:

$$A_1 = \begin{bmatrix} \frac{\partial f_1}{\partial x_1} & \frac{\partial f_1}{\partial x_2} \\ \frac{\partial f_2}{\partial x_1} & \frac{\partial f_2}{\partial x_2} \end{bmatrix}$$

$$= \begin{bmatrix} \ddot{q} & 1 \\ 2\mu\ddot{q} - (w_0^2 + 2k_2\alpha + 3k_3\alpha^2) & 2\mu \end{bmatrix} \tag{19}$$

$$B_1 = \begin{bmatrix} \frac{\partial f_1}{\partial \tau_1} \\ \frac{\partial f_2}{\partial \tau_1} \end{bmatrix} = \begin{bmatrix} 0 \\ 1 \end{bmatrix}$$

By constructing a new state variable $\tilde{x} = (\tilde{x}_k - \tilde{x}_r)/T$ and control variable Δu_k , the state-space equation becomes:

$$\begin{cases} \tilde{\xi}_{k+1} = A \tilde{\xi}_k + B \Delta u_k \\ y_k = C \tilde{\xi}_k \end{cases} \tag{20}$$

In the equation:

$$\begin{aligned}
 A &= \begin{bmatrix} A_1 & B_1 \\ O_{N_u \times N_x} & I_{N_u \times N_u} \end{bmatrix} \\
 &= \begin{bmatrix} \ddot{q} & 1 & 0 \\ 2\mu\ddot{q} - (w_0^2 + 2k_2\alpha + 3k_3\alpha^2) & 2\mu & 1 \\ 0 & 0 & 1 \end{bmatrix} \\
 B &= \begin{bmatrix} B_1 \\ I_{N_u \times N_u} \end{bmatrix} = \begin{bmatrix} 0 \\ 1 \\ 1 \end{bmatrix} \\
 C &= [I_{N_x \times N_x} \quad O_{N_x \times N_u}] = \begin{bmatrix} 1 & 0 & 0 \\ 0 & 1 & 0 \end{bmatrix}
 \end{aligned} \tag{21}$$

Where N_x is the number of state variables, and N_u is the number of control variables. At time instant k :

$$\xi_k = \begin{bmatrix} \xi(k|k) \\ \xi(k+1|k) \\ \xi(k+2|k) \\ \vdots \\ \xi(k+N/k) \end{bmatrix} \Delta u_k = \begin{bmatrix} \Delta u(k|k) \\ \Delta u(k+1|k) \\ \Delta u(k+2|k) \\ \vdots \\ \Delta u(k+N/k) \end{bmatrix} \tag{22}$$

Let the output be $y = \xi$, and the error $E = y - R = \xi - 0 = \xi$ (with the reference point taken as $(x_r, u_r) = (0, 0)$). The cost function is as follows:

$$J = \sum_{i=0}^{N-1} (\xi^T Q \xi + \Delta u^T R \Delta u + \xi k_N^T F \xi k_N) \tag{23}$$

$k_N = (k + N)$

Wherein,

$$\begin{cases} \xi = \xi(k+i|k) \\ \Delta u = \Delta u(k+i|k) \end{cases} \tag{24}$$

Optimal control is achieved by predicting the system's performance over a certain period using a model. Letting $(k|k) = \xi_k$, from expression $\xi_{k+1} = A\xi_k + B\Delta u_k$, we can derive its discrete state-space representation as:

$$\xi_{k+1} = A\xi(k|k) + B\Delta u(k|k) = A\xi_k + B\Delta u_k \tag{25}$$

Similarly, we can obtain:

$$\begin{aligned}
 \xi(k+2|k) &= A\xi(k+1|k) + B\Delta u(k+1|k) \\
 &= A[A\xi_k + B\Delta u(k|k)] + B\Delta u(k+1|k) = A^2\xi_k + AB\Delta u(k|k) + B\Delta u(k+1|k) \\
 \xi(k+N|k) &= A^N\xi_k + A^{N-1}B\Delta u(k|k) + A^{N-2}B\Delta u(k+1|k) + \\
 &\quad \dots + B\Delta u(k+N-1|k)
 \end{aligned} \tag{26}$$

From the above equation, the state-space representation can be derived as:

$$\zeta_k = \begin{bmatrix} I \\ A \\ A^2 \\ \vdots \\ A^N \end{bmatrix} \xi_k + \begin{bmatrix} 0 & 0 & \dots & 0 \\ B & \ddots & 1 & \vdots \\ \vdots & \ddots & \ddots & \vdots \\ A^{N-1}B & \dots & B & 0 \end{bmatrix} \begin{bmatrix} \Delta u(k|k) \\ \Delta u(k+1|k) \\ \vdots \\ \Delta u(k+N|k) \end{bmatrix} \tag{27}$$

Wherein $\zeta = M\xi_k + Cu_k$. Similarly, by simplification, we obtain:

$$\begin{aligned}
 J &= \begin{bmatrix} \xi(k|k) \\ \xi(k+1|k) \\ \vdots \\ \xi(k+N/k) \end{bmatrix} \begin{bmatrix} Q & & & \\ & \ddots & & \\ & & Q & \\ & & & F \end{bmatrix} \begin{bmatrix} \xi(k|k) \\ \xi(k+1|k) \\ \vdots \\ \xi(k+N/k) \end{bmatrix} \\
 &+ \begin{bmatrix} \Delta u(k|k) \\ \Delta u(k+1|k) \\ \vdots \\ \Delta u(k+N|k) \end{bmatrix} \begin{bmatrix} R & & & \\ & \ddots & & \\ & & \ddots & \\ & & & R \end{bmatrix} \begin{bmatrix} \Delta u(k|k) \\ \Delta u(k+1|k) \\ \vdots \\ \Delta u(k+N|k) \end{bmatrix}
 \end{aligned} \tag{28}$$

The cost function of the controller is defined as:

$$J = \zeta_k^T \bar{Q} \zeta_k + \Delta u_k^T \bar{R} \Delta u_k \tag{29}$$

Where \bar{Q} is the control weight matrix, and \bar{R} is the input state weight matrix.

Based on the above, the cost function can be obtained as:

$$J = \xi_k^T G \xi_k + 2\xi_k^T E \Delta u_k + \Delta u_k^T H \Delta u_k \tag{30}$$

Wherein:

$$\begin{cases} G = M^T \bar{Q} M \\ E = M^T \bar{Q} C \\ H = C^T \bar{Q} C + \bar{R} \end{cases} \tag{31}$$

Considering the constraints of the belt drive system, define the constraint range to solve for the minimum value of the cost function:

$$\begin{cases} J_{min} = \xi_k^T G \xi_k + 2\xi_k^T E \Delta u_k + \Delta u_k^T H \Delta u_k \\ X_{min} \leq X_k \leq X_{max} \\ \Delta U_{min} \leq \Delta U_k \leq \Delta U_{max} \end{cases} \quad (32)$$

Control strategies, based on the input-output relationship and dynamic behavior of the system model, are typically represented in state-space or transfer function form. In the control sequence, the first element serves as the actual control input at the current moment, which is then applied to the system and progressively carried out to the next moment [16-19]. Subsequently, based on the state information of the system, future control outputs are re-predicted, and a new sequence of control increments is obtained through optimization. This process iterates continuously until the control task requirements are satisfied. Utilizing this model, Model Predictive Control (MPC) can perform optimized control over the system in a dynamic environment and adjust the system based on real-time feedback, gradually converging to and maintaining the stability of the desired state [20-25].

IV. NUMERICAL SIMULATION AND VALIDATION

To verify the feasibility and control effectiveness of this model control method, numerical simulations and validations were conducted using a belt drive system as the control object. The system parameters are shown in Table 1.

Table 1: Parameters of the Belt Drive System

Drive Wheel Radius r_1	Driven Wheel Radius r_2	New Viscous Damping Coefficient μ	Input Torque M
0.1m	0.2m	1	5N.m

Assuming the prediction horizon is $N = 5$, the state variable weight matrix is $Q = 100I_1$, the terminal weight matrix for state variables is $F = 0.1I_2$, and the input weight matrix is $R = 0.1I_3$. The state constraints for the robotic arm are:

$$\begin{bmatrix} -\pi \\ -5 \end{bmatrix} \leq \xi \leq \begin{bmatrix} \pi \\ 5 \end{bmatrix}, [-100] \leq \Delta u \leq [100] \quad (33)$$

Assuming its initial state is $\xi = [\pi / 3 \ -2]^T$, and the desired final state is $\xi = [0 \ 0]^T$, the simulation results are shown in the figure 5:

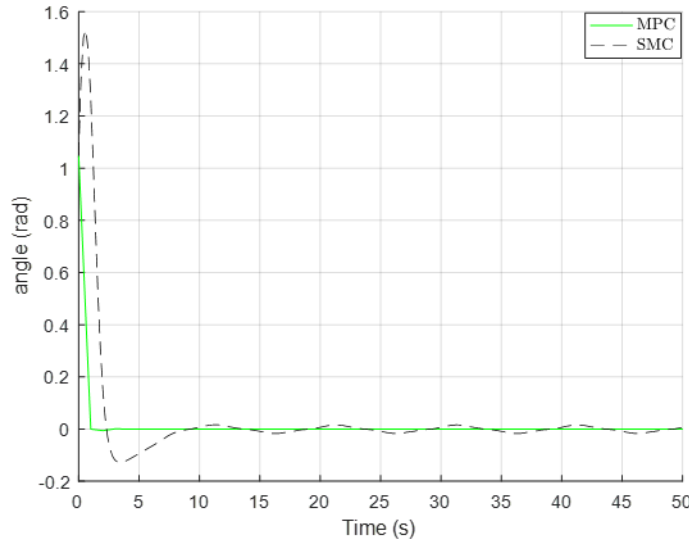


Figure 5: Torsional Angle Variation Curve

As shown in Figure 5, the angle of the belt drive system is displayed. Under Sliding Mode Control (SMC), the torsional angle reaches a peak of 1.5 radians at 0.90 seconds, followed by a series of oscillations, and stabilizes at zero around 6.1 seconds later. In contrast, under Model Predictive Control (MPC), both the torsional angle and its angular velocity approach the desired values more quickly at 1.20 seconds and subsequently stabilize rapidly.

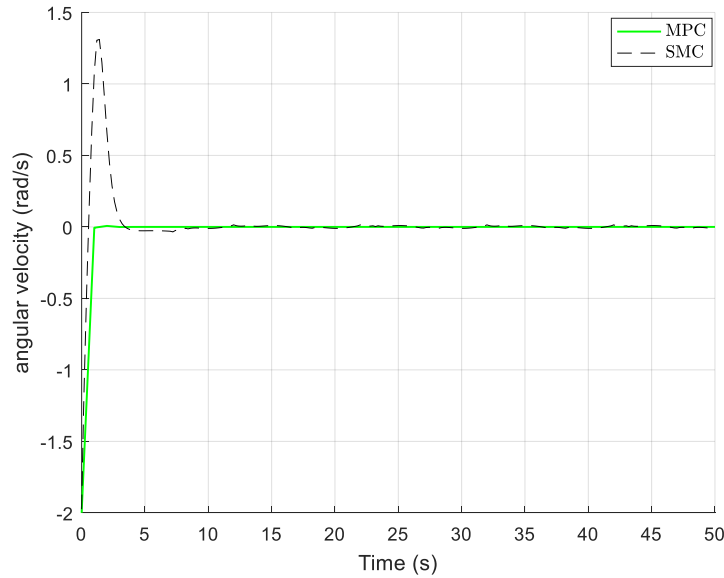


Figure 6: Torsional Angular Velocity Variation Curve

As depicted in Figure 6, the changes in angular velocity of the belt drive system are shown. Under the Sliding Mode Control (SMC) strategy, the torsional angular velocity reaches its maximum value of 1.30 rad/s at 1.80 seconds, followed by a series of oscillations before stabilizing at zero around 3.7 seconds later. In comparison, under the Model Predictive Control (MPC) strategy, both the torsional angle and its angular velocity more rapidly approach the desired values at 1.20 seconds and subsequently achieve stability quickly.

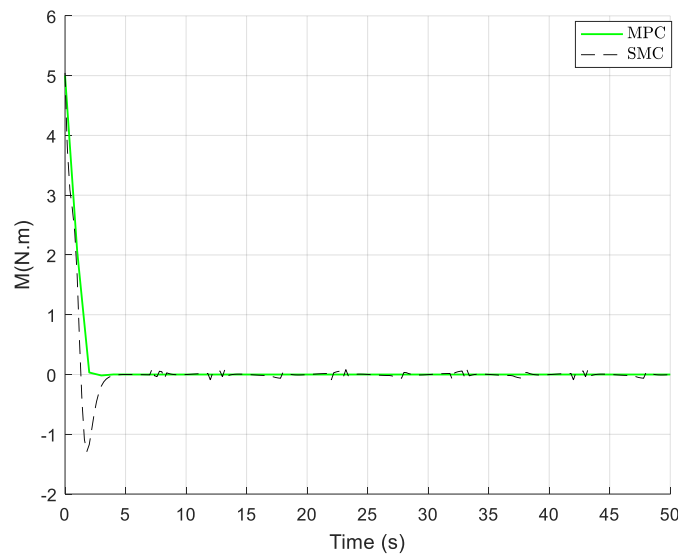


Figure 7: Input Torque Variation Curve

As illustrated in Figure 7, the chart displays the variation of input torque in the belt drive system. Under the influence of the Sliding Mode Control (SMC) strategy, the output torque reaches its peak value of 1.34 N·m at 2.7 seconds, followed by a series of oscillations before finally stabilizing at zero around 5.0 seconds later. In contrast, when the Model Predictive Control (MPC) strategy is applied, the input control variable itself increases as the difference between the system state and the desired state becomes larger. As the system state approaches the desired state, the control variable gradually decreases and ultimately tends to zero. The system's torsional angle and its angular velocity are able to more rapidly approach the desired values in a shorter timeframe, specifically at 2.60 seconds, and subsequently quickly stabilize.

In summation, as delineated in Figures 5-7, it becomes apparent that while Sliding Mode Control (SMC) can facilitate an immediate rapid response, the ensuing oscillatory phase inherent to its operation could potentially compromise system stability and protract the duration required for the system to attain a state of equilibrium. Conversely, Model Predictive Control (MPC), through its predictive analysis of future system behaviors coupled with the optimization of control inputs, exhibits markedly superior performance attributes. This is

particularly evident in its capacity to swiftly achieve and sustain the desired operational state, thereby affirming its pronounced advantage in the management of belt drive systems. By efficaciously diminishing oscillatory tendencies and accelerating system stabilization, MPC furnishes a methodology for precise control that is both more efficacious and reliable, aligning with the stringent demands characteristic of industrial application.

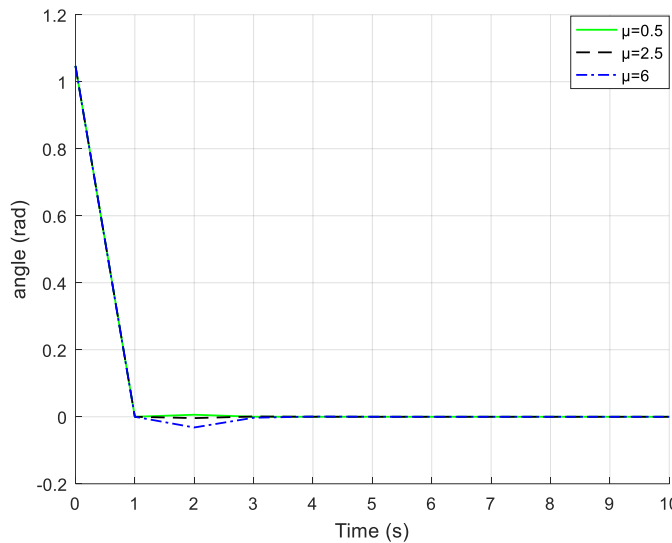


Figure 8: Torsional Angle Variation Curves with Different Time Domain Parameters

As depicted in Figure 8, the torsional angle of the belt drive system exhibits distinct dynamic behaviors under varying time-domain parameters. Specifically, with a time-domain parameter $\mu = 0.5$, the torsional angle decreases from 1.04 radians to zero within the initial second, slightly rises to 0.01 radians in the second, and gradually returns to zero, achieving stability; for $\mu = 2.5$, the torsional angle smoothly transitions from 1.04 radians to zero within one second, demonstrating rapid stabilization; under the condition of $\mu = 6$, the torsional angle initially decreases to zero, followed by a slight negative overshoot to -0.025 radians, and eventually stabilizes within three seconds. These observations highlight that the system exhibits the best dynamic performance at a time-domain parameter of $\mu = 2.5$, including the minimal overshoot, fastest response, and optimal stability, underscoring the importance of appropriately selecting time-domain parameters for optimizing the performance of belt drive systems.

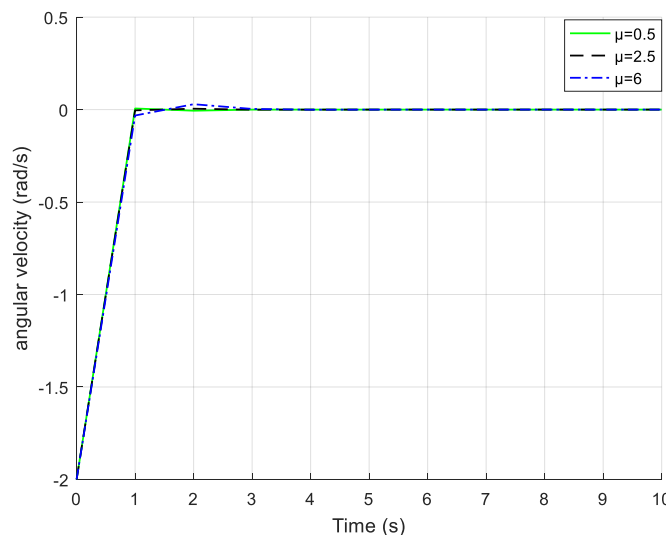


Figure 9: Torsional Angular Velocity Variation Curves with Different Time Domain Parameters

Figure 9 elucidates the torsional angular velocity dynamics of the belt drive system across varying time-domain parameters. Notably, at $\mu = 0.5$, a progression from -2 rad/s to 0.01 rad/s within the initial second, tapering to stability by the third second, is observed. Conversely, at $\mu = 2.5$, a more direct transition from -2 rad/s to a steady state within the same timeframe signifies rapid stabilization. At $\mu = 6$, a swift adjustment to 0 followed by a marginal increase to 0.025 rad/s, and subsequent stabilization, further underscores the differential response across parameters. The system's dynamics under $\mu = 2.5$ —characterized by minimal overshoot and

expedited return to equilibrium—underscore the significance of judicious time-domain parameter selection in optimizing system stability and response efficacy.

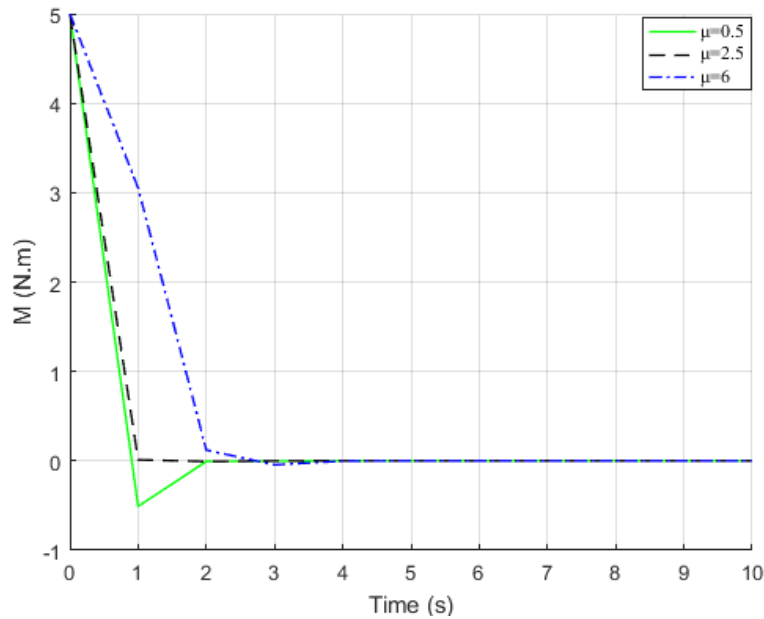


Figure 10: Input Torque Variation Curves under Different Time-Domain Parameters

Figure 10 illustrates the variation in input torque of the belt drive system under different time-domain parameters. With the time-domain parameter $\mu = 0.5$, the torque decreases from 5 N·m to 0.5 N·m within the 0 to 1-second interval and further reduces to zero within the 1 to 2-second interval, achieving stability. For the time-domain parameter $\mu = 2.5$, the angular velocity decreases from 5 N·m to zero within the first second and quickly stabilizes. Meanwhile, for the time-domain parameter $\mu = 6$, the angular velocity rapidly drops from 5 N·m to 0.18 N·m within the 0 to 2-second interval and then decreases to zero in the 2 to 3-second interval. Analysis indicates that under the time-domain parameter $\mu = 2.5$, the system exhibits the least overshoot, the fastest response speed, and optimal stability, emphasizing the critical role of precise time-domain parameter selection in enhancing system performance.

As illustrated in Figures 8-10, the belt drive system's angle, angular velocity, and input torque exhibit distinct characteristic curves at time $\mu = 0.5, 2.5, 6$, among which the vibration range is minimized, the overshoot is the smallest, the response is quicker, and the stability is the best at time $\mu = 2.5$. In summary, elastic damping plays a significant role in influencing the vibrational characteristics of elastic systems. Rational control of damping can effectively adjust the vibration's amplitude, frequency, stability, and response time characteristics.

V. CONCLUSION

This study initially investigated the causes of vibration in belt drive systems, identifying that the main sources stem from the friction among internal components and various disturbances, which collectively trigger low-frequency vibrations within the system. Subsequently, a mathematical model of the belt drive mechanism was constructed using the Lagrangian method, and the Model Predictive Control (MPC) strategy was applied to conduct an in-depth study on the torsional vibration of belt drives. Simulation results demonstrate that the model predictive algorithm exhibits superior performance in suppressing vibrations of the belt drive system. Compared to traditional sliding mode control, the response speeds for tracking torsional position and angular velocity were improved by approximately 2 seconds and 1 second, respectively, effectively reducing system vibrations. Furthermore, as control parameters are adjusted, the system's vibration amplitude, frequency, stability, and response time characteristics will change accordingly. Therefore, the rational selection of control parameters is crucial for achieving vibration suppression in belt drive systems.

DECLARATION OF CONFLICTING INTERESTS

The author(s) declared no potential conflicts of interest with respect to the research, authorship, and/or publication of this article.

ACKNOWLEDGMENT

This research is part of a special project for the construction of the Beijing Tianjin Hebei collaborative innovation community: "Research and application of key technologies of wafer transfer robot in a clean environment" (22341802D).

REFERENCES

- [1] H. H. Pan, K. S. Ding, X. P. Wu, et al. "Suppression of End-Effector Vibration in Industrial Robots Based on Parameter Decoupling Notch Filter." *Machine Tool & Hydraulics*, vol. 51, 2023, pp. 1-6.
- [2] H. Liu, L. J. Jiang, Q. Chen. "Research and Application of Vibration Suppression Method for High-Speed Motion Positioning of Industrial Robots." *China New Technologies and Products*, vol. 22, 2022, pp. 20-23.
- [3] J. Y. Hu, X. Han, Y. R. Tao, et al. "Reliability Analysis of Residual Vibration Suppression in Flexible Servo Systems under S-curve Trajectory with Bounded Uncertainty " *Journal of Mechanical Engineering*, vol. 59, 2023, pp. 1-10.
- [4] T. Zhang, Z. Y. Li, Y. B. Zou. "Research on Residual Vibration Suppression and Measurement Method of Flexible Load for Robots." *Mechanical Design and Manufacturing*, vol.22, 2022, pp. 225-229.
- [5] D. Shin, K. J. Yun, "Improvement of Vibration Performance for Wafer Transfer Robot using Frequency Analysis of Motion Profile." *Journal of the Korean Society for Precision Engineering*, vol. 31, 2014, pp. 697-703.
- [6] W. Aribowo, K. Terashima. "Cubic Spline Trajectory Planning and Vibration Suppression of Semiconductor Wafer Transfer Robot Arm." *International Journal of Automation Technology*, vol. 8, 2014, pp. 265-274.
- [7] Oh-Hara S, Hirata K, Ohta Y. "A switching gain scheduled approach for wafer transfer robots and its experimental evaluations," *American Control Conference. IEEE*, 2006, pp. 3898-3903.
- [8] T. G. Liu, L. Chang. "Application of MPC Algorithm Based on Offset Control in Pre-Twisted Blade Vibration Control." *Journal of Vibration and Shock*, vol. 38, 2019, pp. 172-177.
- [9] Q. J. Xiong. "Trajectory Tracking Algorithm for Robotic Arms Based on Model Predictive Control." *Industrial Technology Innovation*, vol. 08, 2021, pp. 47.
- [10] H. Wang, X. Y. Meng, C. X. Li. "Design of UAV Trajectory Tracking Controller Based on MPC." *Systems Engineering and Electronics*, vol. 43, 2021, pp. 191-198.
- [11] R. Z. Qi, L. Ding. "Adaptive Fractional-Order Terminal Sliding Mode Control for Rope-Driven Aerial Manipulators," *Journal of Electronic Measurement and Instrumentation*, vol. 37, 2023, pp. 206-212.
- [12] Q. J. Xiong. "Trajectory Tracking Algorithm for Robotic Arms Based on Model Predictive Control," *Industrial Technology Innovation*, vol. 08, 2021, pp.47-53.
- [13] H. Wu, Y. Tan, X. L. Guo, X. T. Mao. "Trajectory Tracking Control of Flexible Joint Space Manipulator Based on Model Predictive Control," *Space Control Technology and Applications*, vol. 45, 2019, pp. 35-41.
- [14] Y. Y. Luo, Y. Mei, M. H. Jiang. "Research on Anti-Sway Control of Photovoltaic Cleaning Robots Based on MPC," *Sensors and Micro Systems*, vol. 42, 2023, pp. 44-47.
- [15] ZHOU K Z L X C L J. "UAV Swarm Formation Reconfiguration Control Based on Variable-Stepsize MPC-APCMPIO Algorithm," *Science China (Information Sciences)*, vol. 66, 2023, pp. 222-243.
- [16] H.A. I A K "Longitudinal and Lateral Control of Vehicle Platoons Using Laguerre-based and Robust MPC with Merge and Exit Maneuvers," *Control Engineering Practice*, vol. 142, 2024, pp.21-32.
- [17] Mohammed V M E L H E. "A Novel Robust Adaptive Neuro-Sliding Mode Steering Controller for Autonomous Ground Vehicles," *Robotics and Autonomous Systems*, vol. 170, 2023, pp.18-29.
- [18] Hongjie J X T X L. "Robust Constraint Satisfaction and Stability of Virtually Coupled Train Set with Uncertain Dynamics: A Dual-Mode Robust MPC Approach," *Transportation Research Part C*, vol. 156, 2023, pp.9-20.
- [19] Xuan D Y R C Q Y. "Push Recovery Control Based on Model Predictive Control of Hydraulic Quadruped Robots," *Journal of Intelligent Robotic Systems*, vol. 109, 2023, pp20-28.
- [20] Gang Y K H X Z. "Nonlinear Disturbance Observer-Based Robust Predefined Time Tracking and Vibration Suppression Control for the Rigid-Flexible Coupled Robotic Mechanisms with Large Beam-Deformations," *Computers and Mathematics with Applications*, vol. 148, 2023, pp. 1-25.
- [21] Shigeo K M. "Reference Input Design of Dual-Mode Vibration Suppression Control for 2DOF Horizontal Robot Arm," *The Proceedings of the International Conference on Motion and Vibration Control*, vol. 20, 2020, pp.1-12.
- [22] Xiaoning K Z M J H W. "Robust adaptive three-dimensional trajectory tracking control for unmanned underwater vehicles with disturbances and uncertain dynamics," *Ocean Engineering*, vol. 289, 2023, pp.13-18.
- [23] Yanfeng J X Y Z Z. "A day-ahead operation regulation method for solar water heating based on model predictive control," *Energy Buildings*, vol. 301, 2023, pp1-15.
- [24] Yifan Y S J Z Y. "Robust MPC-based trajectory tracking of autonomous underwater vehicles with model uncertainty," *Ocean Engineering*, vol. 286, 2023, pp.8-19.
- [25] Yonghwan J. "Integrated Vehicle Controller for Path Tracking with Rollover Prevention of Autonomous Articulated Electric Vehicle Based on Model Predictive Control," *Actuators*, vol. 12, no. 1, 2023, pp. 41-41.